The impact of gaseous degradation on the gas–particle partitioning of methylated polycyclic aromatic hydrocarbons

Fu-Jie Zhu[a,b,c], Zi-Feng Zhang[a,b], Li-Yan Liu[a,b], Pu-Fei Yang[a,b], Peng-Tuan Hu[a,d], Geng-Bo Ren[c], Meng Qin[a,b], Wan-Li Ma [a,b,*]

[a] International Joint Research Center for Persistent Toxic Substances (IJRC-PTS), State Key Laboratory of Urban Water Resource and Environment, Harbin Institute of Technology, Harbin 150090, China

[b] Heilongjiang Provincial Key Laboratory of Polar Environment and Ecosystem (HPKL-PEE), Harbin 150090, China

[c] School of Energy and Environmental Engineering, Hebei University of Technology, Tianjin 300401, China

[d] School of Environment, Key Laboratory for Yellow River and Huai River Water Environment and Pollution Control, Ministry of Education, Henan Normal University, Xinxiang 453007, China

*Corresponding author. International Joint Research Center for Persistent Toxic Substances (IJRC-PTS), State Key Laboratory of Urban Water Resource and Environment, Harbin Institute of Technology, 73 Huanghe Road, Nangang District, Harbin 150090, Heilongjiang, China.
Email address: mawanli002@163.com

Abstract

The partitioning of semi-volatile organic compounds (SVOCs) between gas and particle phases plays a crucial role in their long-range transport and health risk assessment. However, the accurate predicting of the gas–particle (G–P) partitioning quotient (K_P') remains a challenge, especially for the light molecular weight (LMW) SVOCs due to their upward deviation from the equilibrium state. In this study, the phenomenon with the influence of gaseous degradation on G–P partitioning was observed. Based on the diurnal study of concentrations and K_P' values for methylated polycyclic aromatic hydrocarbons (Me-PAHs), it was found that the K_P' values of methylated naphthalenes (Me-Naps, one type of LMW SVOCs) during daytime were higher than that during nighttime, and the regression lines of log K_P' versus log K_{OA} (octanol-air partitioning coefficient) for daytime and nighttime were non-overlap, which were different with other Me-PAHs. Compared with other diurnal influencing factors, the higher gaseous degradation of Me-Naps in the daytime than that in the nighttime should partially explain their special diurnal variation of K_P', which provided a new explanation for the non-equilibrium behavior of K_P' of LMW SVOCs. Moreover, the influence of gaseous degradation on the deviation of K_P' from the equilibrium state was deeply studied based on the steady-state G–P partitioning model that considering particulate proportion in emission (ϕ_0). The increasing times of K_P' influenced by the gaseous degradation deviated from the equilibrium state can be calculated by $1 + 13.2\phi_0 \times k_{deg}$ (gaseous degradation rate). The K_P' increase along with the increasing of k_{deg} proved that higher gaseous degradation in the daytime could increase K_P' value. Furthermore, an amplification of K_P' ranging from 1.10 to 5.58 times (90% confidence interval: 1.01 to 14.4) under different ϕ_0 (0 to 1) in the temperature range of −50 to 50°C was estimated by the Monte Carlo Analysis. In summary, it can be concluded that the influence of

gaseous degradation should also be considered for the G–P partitioning models of SVOCs, especially for the LMW SVOCs, which provided new insights into the related fields.

Keywords: Equilibrium state; Upward deviation; Light molecular weight SVOCs; Diurnal variation; Methylated polycyclic aromatic hydrocarbons

Graphic abstract

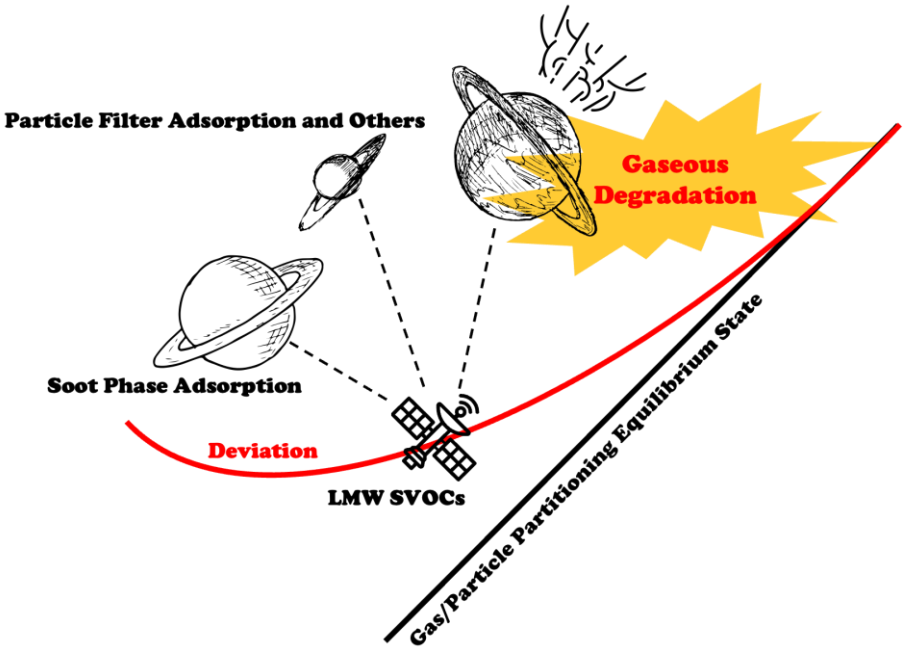

1. Introduction

The partitioning of semi-volatile organic compounds (SVOCs) between gas and particle phases, known as gas–particle (G–P) partitioning, is a crucial process for their long-range atmospheric transport (Li et al., 2020; Zhu et al., 2021b) and their entry pathway into the human body (Hu et al., 2021). To investigate the G–P partitioning mechanism of SVOCs, researchers have widely employed the correlation between the G–P partitioning coefficient (K_P) at equilibrium state and the octanol-air partition coefficient (K_{OA}) (Ma et al., 2019; Harner and Bidleman, 1998). The prediction of K_P based on K_{OA} was conducted in previous studies, which deduced some G–P partitioning models (Qiao et al., 2020). The Harner-Bidleman (H-B) model (Harner and Bidleman, 1998) and the Dachs-Eisenreich (D-E) model (Dachs and Eisenreich, 2000) were successfully applied in the prediction of K_P for different SVOCs using the equilibrium-state theory (Wang et al., 2011; Sadiki and Poissant, 2008). In addition, the Li-Ma-Yang (L-M-Y) model (Li et al., 2015) was established based on the steady-state theory, which exhibited good performance for predicting the G–P partitioning quotient (K_P') at steady state, particularly for high molecular weight (HMW) SVOCs (Qiao et al., 2020; Li et al., 2017; Hu et al., 2020).

Previous studies had found that the K_P' deviated from the equilibrium state for both HMW SVOCs (i.e., high log K_{OA} value) (Li et al., 2015; Li and Jia, 2014) and light molecular weight (LMW) SVOCs (Ma et al., 2020; Dachs and Eisenreich, 2000). For the HMW SVOCs, the particulate SVOCs were either deposited or removed through dry and wet depositions of particles before reaching equilibrium state, as demonstrated by both the theoretical study (L-M-Y model) and the monitoring study (Mackay et al., 2019; Li et al., 2015), which can be used to explain the deviation. For the LMW SVOCs, the K_P' deviated upward from the equilibrium state, and the deviation could be multiple

orders of magnitude, such as LMW polycyclic aromatic hydrocarbons (PAHs) (Ma et al., 2020; Ma et al., 2019). Several explanations have been proposed for this deviation. First, the artifacts resulting from the adsorption of gaseous PAHs onto particle filters during atmospheric sampling can increase K_P' values (Zhang and Mcmurry, 1991; Hart et al., 1992; Hart and Pankow, 1994). In an early study, the double filters sampling method demonstrated that gas adsorption onto filters would cause an overestimation of K_P' by a factor of 1.2 to 1.6 times (Hart and Pankow, 1994). However, the overestimation is much lower than the deviation with multiple orders of magnitude. Second, the enhanced adsorption of gaseous SVOCs onto various phases (e.g., soot phase and inorganic phases) within particles has been extensively documented (Shahpoury et al., 2016; Dachs and Eisenreich, 2000). Some G–P partitioning models were established with the consideration of the enhanced adsorption, such as the D-E model and the poly-parameter linear free energy relationships (pp-LFER) model (Shahpoury et al., 2016; Dachs and Eisenreich, 2000). However, these models cannot fully explain the deviation from the equilibrium state for the LMW SVOCs, such as some LMW PAHs (acenaphthylene (Acy), acenaphthene (Ace), and fluorene (Flu)) (Ma et al., 2020).

A recent study delved into the non-equilibrium interplay of G–P partitioning resulting from chemical reactions of SVOCs (Wilson et al., 2020). The study found that when the chemical loss of SVOCs in the gas or particle phase exceeded the replenishment from the particle or gas phase, the K_P' values could deviate from the equilibrium state (Wilson et al., 2020). According to the findings, the upward deviation of LMW SVOCs from the equilibrium state might be caused by the faster chemical loss of SVOCs in the gas phase than the replenishment from the particle phase. However, further studies are required to confirm this hypothesis. Our previous study provided

new insights into the deviation from the equilibrium state for several LMW PAHs by studying the diurnal variation of K_P' values (Zhu et al., 2022). The study found that the K_P' values for the three LMW PAHs (Acy, Ace, and Flu) were higher in the daytime than those in the nighttime (Zhu et al., 2022). In addition, the chemical reactions of SVOCs were different between the daytime and nighttime (Ohura et al., 2013). Therefore, the study on the diurnal variation of G–P partitioning between the daytime and nighttime can be considered as a special case for deep understanding the deviation of LMW SVOCs from the equilibrium state.

In order to comprehensively investigate the deviation of the K_P' value from the equilibrium state for LMW SVOCs, the diurnal variation of concentrations and K_P' values for methylated PAHs (Me-PAHs) was conducted in this study. Furthermore, the influence of the gaseous degradation on the deviation of K_P' from the equilibrium state was quantified based on the theoretical model for both LMW Me-PAHs and PAHs, which provided new insights into the G–P partitioning of SVOCs.

2. Materials and methods

2.1. Sampling method

The detailed information for the sampling method and site can be found in our previous study (Zhu et al., 2022; Zhu et al., 2021a). In brief, the sampling program was conducted at an urban location on the rooftop of a 14-meter-high building in Harbin City in northeastern China. Harbin City has an obvious seasonal variation, with the heating season from 20th October to 20th April and the non-heating season from 20th April to 20th October. A total of 32 pairs of air samples during daytime (9:00 a.m. to 5:00 p.m.) and nighttime (9:00 p.m. to 5:00 a.m.) were collected every 10 days from December 2017 to November 2018, which minimized the impact of heavy traffic. The

glass fiber filters (GFFs) and polyurethane foam plugs (PUFs) were used to collect particulate and gaseous samples, respectively, using a high-volume air sampler (TE-1000, Tisch Environmental, Ohio, USA) with an air flow rate of 0.24 std m^3/min. The GFFs and PUFs were carefully sealed and stored in a refrigerator at −20℃ prior to treatment.

2.2. Analysis procedure of Me-PAHs

The analysis procedure for Me-PAHs was identical to that of PAHs (Zhu et al., 2022; Zhu et al., 2021a). In brief, the Soxhlet extraction and active silica gel column were used to extract and purify the GFFs and PUFs samples. Prior to extraction, four surrogates (naphthalene-D8, fluorene-D10, pyrene-D10, and perylene-D12) were added to all samples. The extractions were then solvent-exchanged into isooctane, concentrated to 1 mL in GC vials with 200 ng quantitation standard (phenanthrene-D10). A total of 49 Me-PAHs were analyzed by an Agilent 7890B gas chromatograph coupled with an Agilent 5977 mass spectrometer detector, with the electron-impact ionization and selected ion monitoring mode. Chromatographic resolution was achieved with a DB-5 MS capillary chromatographic column (60 m × 0.25 mm i.d. × 0.25 μm film thickness, J&W Scientific). Ultrapure helium gas (>99.9999%) was used as the carrier gas at a constant flow rate of 1 mL/min. An aliquot (2 μL) of the sample was injected into the multi-mode inlet of the GC/MS at 280℃ via the pulsed splitless mode. The column-oven temperature program was as follows: hold at 100℃ for 1 min, ramp to 200℃ at 40℃ /min, hold for 13 min, ramp to 300℃ at 80℃ /min, hold for 22 min, ramp to 310℃ at 50℃ /min, hold for 11 min with the post run of 310℃, hold for 3 min. The transfer line temperature was maintained at 280℃. For the mass spectrometer, the MS source and quadrupole temperatures were set at 230℃ and 150℃, respectively. Detailed information and mass spectrometry parameters for the 49 Me-

PAHs are summarized in **Table S1, supporting information (SI)**. A representative chromatogram is depicted in **Fig. S1, SI**.

2.3. Quality assurance/quality control

In order to minimize the errors, rigorous quality assurance/quality control procedures were implemented in the present study. Prior to sampling, GFFs were subjected to a cleaning process involving baking at 450℃ for 6 hours, while PUFs were extracted via Soxhlet extraction using dichloromethane for 24 hours and hexane for an additional 24 hours. All glassware utilized in the experimental process was cleaned with dichloromethane and hexane prior to use. Field blanks were conducted on a monthly basis, and laboratory blanks were added for every 11 samples. The quantitation standard was utilized to correct fluctuations of the corresponding instrument signal. The average recoveries of the four surrogates ranged from 70% to 110% for all samples, which were deemed acceptable for the utilization of concentration data without correction via surrogate recoveries. The instrument detection limit (IDL) was calculated as three times of the signal to noise, with IDLs for all Me-PAHs ranging from 0.0154 ng to 0.951 ng (**Table S1, SI**), utilizing a constant injection volume of 2 μL. Concentrations below IDLs were excluded from further calculations. The recoveries of all Me-PAHs with spiked blank samples ranged from 94% to 107%. The final reported concentrations were corrected by the blanks, but not corrected with recoveries of spiked blank samples and surrogates. A five-point calibration curve was established using concentrations of 5, 10, 50, 100, and 500 ng/mL, with a correlation coefficient (r^2) exceeding 0.99.

2.4. G–P partitioning quotient

The K_P' ($m^3/\mu g$) was calculated based on the following equation:

$$K_P' = C_P/(C_G \times TSP) \quad (1)$$

where, C_P and C_G are the concentrations (ng/m^3) of Me-PAHs in the particle phase and gas phase, respectively; and *TSP* is the concentration of the total suspended particles in air (μg/m^3).

In general, the value of log K_{OA} can be calculated using the following equation:

$$\log K_{OA} = A + B/T \quad (2)$$

where, *T* is the ambient temperature (K); *A* and *B* are constants.

For most Me-PAHs, the values of *A* and *B* were estimated through the utilization of the pp-LFER equation, which relied on the solute descriptors obtained from the UFZ-LSER database (Baskaran et al., 2021; Ulrich et al., 2017). The calculation methods and corresponding parameters have been concisely summarized in **Tables S2 and S3, SI**. By utilizing the values of *A* and *B*, the value of K_{OA} for Me-PAHs can be obtained by Eq. (2) at any temperature.

2.5. Data analysis method

The statistical analysis was conducted using the SPSS Software (Version 24.0). Prior to analysis, the normal distribution test was performed via the One-Sample Kolmogorov-Smirnov Test. The Paired Sample t-test was utilized for difference analysis in datasets exhibiting normal distribution, while the Wilcoxon Signed Rank Test was employed for the non-normal distribution datasets. Results were considered as statistically significant if the *p*-value was less than 0.05.

3. Results and discussion

3.1. Diurnal variation of concentration

Among the 49 Me-PAHs, 30 Me-PAHs were frequently detected with detection rates exceeding 30% (**Table S1, SI**), and they were considered for further discussion.

As depicted in **Fig. 1a**, the total concentrations of 30 Me-PAHs (ΣMe-PAHs) in total phase (particle phase + gas phase) were compared between daytime and nighttime in different seasons. A clear diurnal variation with higher concentrations of Me-PAHs during nighttime as compared to daytime was observed. The geometric mean (GM) concentrations (range of 25th% to 75th%) of ΣMe-PAHs were 12.0 ng/m^3 (4.51 to 34.6 ng/m^3) and 23.6 ng/m^3 (7.97 to 69.9 ng/m^3) in daytime and nighttime, respectively. Furthermore, the concentrations of ΣMe-PAHs in total phase during nighttime were significantly higher than those during daytime ($p < 0.05$), with the GM value of nighttime/daytime (N/D) ratios of 1.97 for the whole sampling period. Although studies on the diurnal variation of Me-PAHs are limited, similar diurnal variations have also been observed in some previous studies for other PAHs, such as PAHs, chlorinated-PAHs, nitrated-PAHs, and oxygenated-PAHs (Cao et al., 2018; Ohura et al., 2013; Zhang et al., 2018; Zhu et al., 2022). It was found that the diurnal variations of emission sources, emission intensity, atmospheric reactions, and meteorological effects were responsible for the diurnal variation of SVOCs concentrations (Ohura et al., 2013; Zhang et al., 2018).

Moreover, it is noteworthy that distinctly diurnal variations were observed among different phases (gas and particle) and different seasons (heating and non-heating) (**Fig. 1b and Fig. 1c**). Notably, a significant increase of concentrations during nighttime compared to that during daytime was observed for the gas phase ($p < 0.01$), while no significant diurnal variation was observed for the particle phase in all seasons and in heating season. Additionally, the N/D ratios were higher in the non-heating season compared to the heating season. For instance, in the non-heating season, the GM N/D ratios were 2.14 and 2.15 for the total and gas phases, respectively. However, in the heating season, the GM N/D ratios were 1.80 and 1.96 for the total and gas phases,

respectively. These findings suggested that gaseous Me-PAHs exhibited more obviously diurnal variation than particulate Me-PAHs, and Me-PAHs in the non-heating season displayed more prominent diurnal variation than that in the heating season.

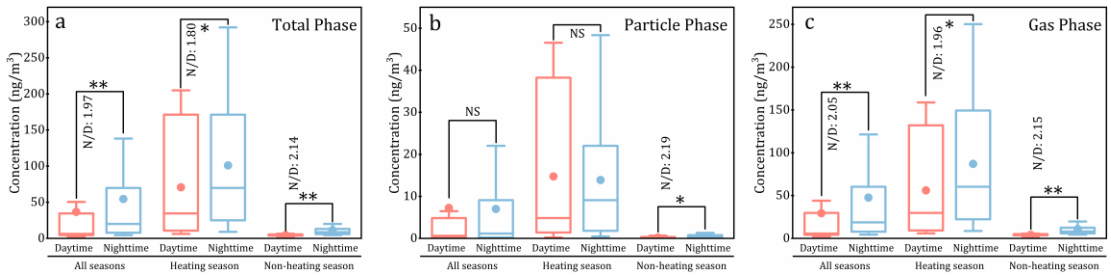

Fig. 1. Comparison with the concentrations of the ΣMe-PAHs between daytime and nighttime in different seasons for different phases (Note: * and ** represent that the differences are significant at 0.05 level and 0.01 level, respectively; NS represents no significant difference; N/D represents the geometric mean value of nighttime/daytime ratio for concentration.)

Furthermore, it is interesting to note that individual Me-PAHs also exhibited different diurnal variations. The N/D ratios, and the GM values of N/D ratios for individual Me-PAHs are presented in **Table S4 and Fig. S2, SI**. The GM values of N/D ratios varied considerably among different Me-PAHs, ranging from 0.347 to 7.30. Regarding to the seasonal differences in diurnal variation (**Table S4, SI**), the results for most individual Me-PAHs were consistent with those for ΣMe-PAHs, with higher GM values of N/D ratios in the non-heating season than the heating season. With respect to the phase differences in diurnal variation (**Table S4 and Fig. S2, SI**), the GM values of N/D ratios in the gas phase for Me-naphthalenes (Me-Naps, one type of LMW SVOCs) were higher than those in the particle phase for individual Me-Naps in all seasons. This result with Me-Naps was consistent with that of ΣMe-PAHs, which could be attributed to the high contribution of Me-Naps to ΣMe-PAHs (mean value: 63%). However, for other Me-PAHs (**Table S4 and Fig. S2, SI**), the N/D ratios in the particle phase were similar or even a little higher than those in the gas phase.

3.2. Diurnal variation of G–P partitioning

In general, the different diurnal variations with the concentrations of SVOCs between the gas phase and particle phase could cause the diurnal variations of K_P' values. As depicted in **Fig. 2**, compared with other Me-PAHs, several LMW Me-PAHs (such as Me-Naps) exhibited significantly higher log K_P' values in the daytime compared to the nighttime ($p < 0.05$). However, the other Me-PAHs, like 3-MeBcP, 5&6&4-MeChr, and 3&5-MeBaA, had higher log K_P' values in the nighttime than those in the daytime ($p < 0.05$). The special diurnal variations of the log K_P' of Me-Naps can be attributed to the different diurnal variations of their concentrations between the two phases. For example, the N/D ratios of concentrations in the gas phase were significantly higher than those in the particle phase for Me-Naps, which was different from other Me-PAHs (**Fig. S2, SI**).

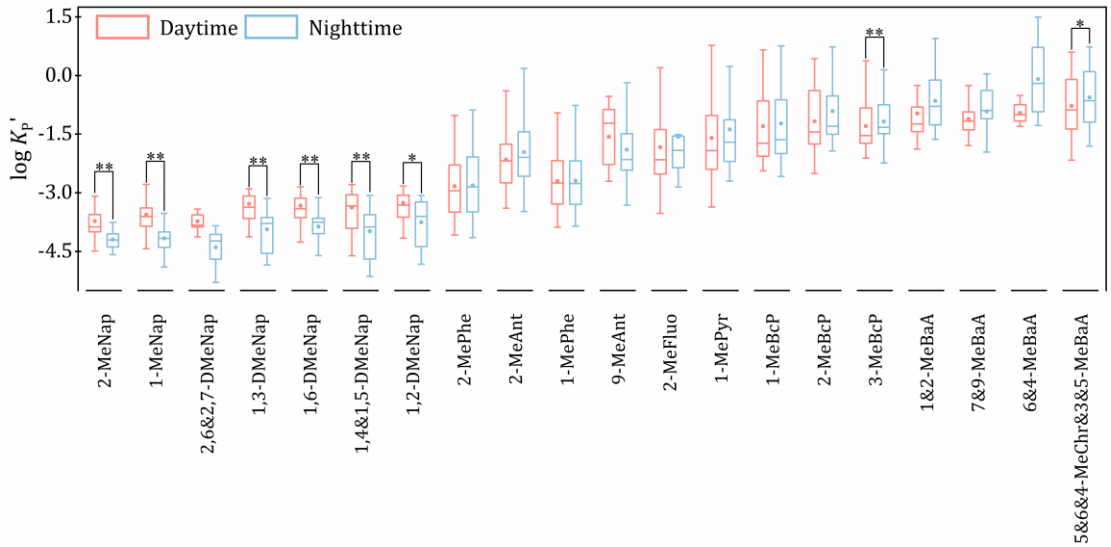

Fig. 2. Comparison of the values of log K_P' for individual Me-PAHs between daytime and nighttime (Note: * and ** represent that the differences are significant at 0.05 and 0.01 level, respectively.)

In order to deeply investigate the diurnal variations of G–P partitioning quotient, the regression lines of log K_P' against log K_{OA} were compared between daytime and nighttime. In general, the diurnal variations were also observed for the relationships

between log K_P' and log K_{OA} for Me-Naps. Interestingly, for these Me-Naps, the regression lines also had obvious diurnal variations as being higher during daytime compared to nighttime (**Fig. 3**). In contrast, no significant differences were observed in the regression lines for the total Me-PAHs (**Fig. S3, SI**) and other individual Me-PAHs (**Fig. S4, SI**) between daytime and nighttime. Given the lower ambient temperatures during nighttime, higher K_P' values during nighttime compared to daytime and the overlap of the two regression lines between daytime and nighttime were expected, just like the total Me-PAHs (**Fig. S3, SI**) and other individual Me-PAHs (**Fig. S4, SI**). However, the different phenomenon with the regression lines of log K_P' against log K_{OA} was observed for Me-Naps (**Fig. 3**).

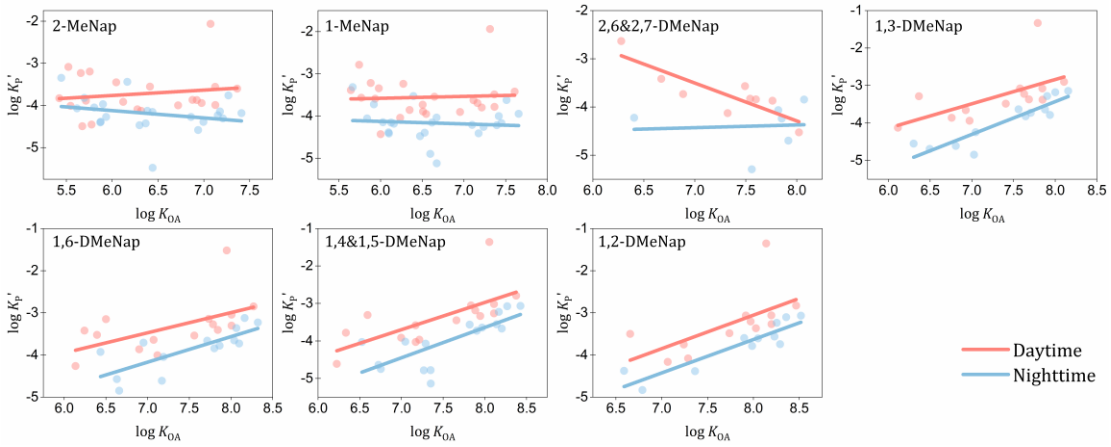

Fig. 3. The regression lines of log K_P' against log K_{OA} between daytime and nighttime for Me-Naps

The specific relationships with concentrations between daytime and nighttime for these Me-Naps can be elucidated by the following equation:

$$C_{P,N}/C_{P,D} < C_{G,N}/C_{G,D} \rightarrow C_{P,N}/C_{G,N} < C_{P,D}/C_{G,D} \quad (3)$$

where, $C_{P,N}$ and $C_{P,D}$ are the particulate concentrations during nighttime and daytime, respectively; $C_{G,N}$ and $C_{G,D}$ are the gaseous concentrations during nighttime and daytime, respectively.

In addition, no significant difference was observed for *TSP* concentrations between daytime and nighttime (GM: 94.5 μg/m^3 in the daytime and 90.5 μg/m^3 in the nighttime). Therefore, the following relationship can be derived:

$$C_{P,N}/C_{G,N}/TSP_N < C_{P,D}/C_{G,D}/TSP_D \rightarrow K'_{P,N} < K'_{P,D} \quad (4)$$

where, TSP_N and TSP_D are the *TSP* concentrations during nighttime and daytime, respectively; $K'_{P,N}$ and $K'_{P,D}$ are the K_P' values during nighttime and daytime, respectively.

When Eqs. (3), and (4) were considered together, it can be found that the higher N/D ratios of concentrations in the gas phase than those in the particle phase could cause higher K'_P values during daytime than those during nighttime. Therefore, the higher log K_P' values in the daytime than the nighttime for Me-Naps (**Fig. 2**) can be explained by the findings with the values of N/D ratios between particle phase and gas phase (**Fig. S2 in SI**). The clarification of the influence factors in the special diurnal variation of the concentrations of these Me-Naps, would help to understand the diurnal variation of G–P partitioning of LMW SVOCs.

As noted in previous studies, the concentrations of SVOCs are influenced by emission intensity, atmospheric reactions, and meteorological effects (Ohura et al., 2013; Zhang et al., 2018). In general, emission intensity can impact the concentration of SVOCs in the total phase (gas phase plus particle phase), while they cannot affect the distribution between the two phases when the steady state has been reached. In other words, this factor cannot cause the diurnal variation of the G–P partitioning for Me-Naps. Among meteorological parameters, temperature is the key factor on the G–P partitioning of SVOCs, which could result in the higher K_P' values during nighttime than those during daytime. However, the opposite results were observed for Me-Naps in this study, which suggested the influences of other factors. As mentioned in previous

studies, the higher atmospheric reactions in the daytime resulted in the lower concentrations of SVOCs in the daytime than those in the nighttime (Ohura et al., 2013; Reisen and Arey, 2005), which might also be responsible for the special diurnal variations of the K_P' values of Me-Naps. Previous studies also suggested that when the rate of chemical loss is faster than the process of G–P partitioning (or the degradation in the gas phase exceeded the replenishment from the particle phase), the G–P partitioning maybe deviate from the equilibrium state (Wilson et al., 2020). In addition, the value of K_P' increased along with the increase of the chemical loss rate (Wilson et al., 2020). Therefore, it can be concluded that the higher gaseous degradation during daytime than that during nighttime might result in higher K_P' values during daytime. The observation of the higher K_P' for these Me-Naps in the daytime than those in the nighttime provided the new insight into the deviation of K_P' from the equilibrium state for LMW SVOCs.

3.3. Influence of gaseous degradation on K_P' of LMW SVOCs

In this section, the new steady-state G–P partitioning model (Zhu et al., 2023) was applied for better understanding the impact of gaseous degradation on the deviation of K_P' from equilibrium state. Based on the model, for the LMW SVOCs, the K_P' values can be obtained using the following simplified equation, and more detailed information about the equation were presented in **Text S1, SI**:

$$\log K'_{\mathrm{P-NS}} = \log K_{\mathrm{P-HB}} + \log(1 + 13.2\phi_0 \times k_{\mathrm{deg}}) \quad (5)$$

where, $K'_{\mathrm{P\text{-}NS}}$ is the predicted G–P partitioning quotient of the new steady-state G–P partitioning model; $K_{\mathrm{P\text{-}HB}}$ is the G–P partitioning coefficient calculated from the H-B model (the equilibrium-state model, $\log K_{\mathrm{P\text{-}HB}} = \log K_{\mathrm{OA}} + \log f_{\mathrm{OM}} - 11.91$, f_{OM} is the organic matters in the particles) (Harner and Bidleman, 1998); ϕ_0 is the particulate

proportion of SVOCs in emission; k_{deg} is the degradation rate of SVOCs in gas phase (h^{-1}).

Based on Eq. (5), the value of K_P' will increase along with the increasing of k_{deg}. As we mentioned above, the gaseous degradation in the daytime was higher than those in the nighttime. Therefore, the application of Eq. (5) can demonstrate that the gaseous degradation of Me-Naps could be part of reason for the higher K_P' in the daytime than that in the nighttime.

Furthermore, the deviation with K_P' from the equilibrium state (log $K_{P\text{-}HB}$) caused by the gaseous degradation for LMW SVOCs can be estimated using the equation of log $(1 + 13.2\phi_0 \times k_{deg})$, which was related to k_{deg} and ϕ_0. The k_{deg} values under 25℃ for the Me-Naps and the three LMW PAHs (Acy, Ace, and Flu) were calculated using their half-lives from the Estimation Programs Interface (EPI) Suite (**Table S5, SI**). Then, the k_{deg} values under different temperature (−50 and 50℃) were calculated using the following equation:

$$k_{\mathrm{deg}\_T} = k_{\mathrm{deg}\_0}\exp\left(\frac{E_{aA}}{R\left(\frac{1}{T_0}-\frac{1}{T}\right)}\right) \quad (6)$$

where, k_{deg_T} is the k_{deg} value at temperature T; k_{deg_0} is the k_{deg} value at 25℃; E_{aA} is the activation energy in air (J/mol); R is the universal gas constant (8.314 J·K/mol); T and T_0 (25℃) are temperature (K). The minimum and maximum k_{deg} values for these PAHs under different temperature were summarized in **Table S5, SI**.

The increasing times of K_P' influenced by the gaseous degradation deviated from the equilibrium state can be calculated based on the equation: $1 + 13.2\phi_0 \times k_{deg}$. To evaluate the impact of the gaseous degradation on the K_P' deviated from equilibrium state, the sensitivity analysis at condition of −50℃ and 50℃ was separately conducted by the Monte Carlo Analysis with 100 000 trials employing the commercial software package Oracle Crystal Ball. Consequently, the range of the impact resulting from the

gaseous degradation was calculated for individual PAHs, and the results are presented in **Fig. 4**. It can be found that, the mean impact caused by the gaseous degradation on K_P' deviation for these PAHs were in the range of 1.10 to 1.98 times (90% confidence interval: 1.01 to 3.89) (**Fig. 4a**) and in the range of 1.54 to 5.58 times (90% confidence interval: 1.04 to 14.4) (**Fig. 4b**) at −50℃ and 50℃, respectively. The influence from the gaseous degradation on the deviation of K_P' from the equilibrium state could approach to one order of magnitude, which cannot be ignored in the study of G–P partitioning of SVOCs.

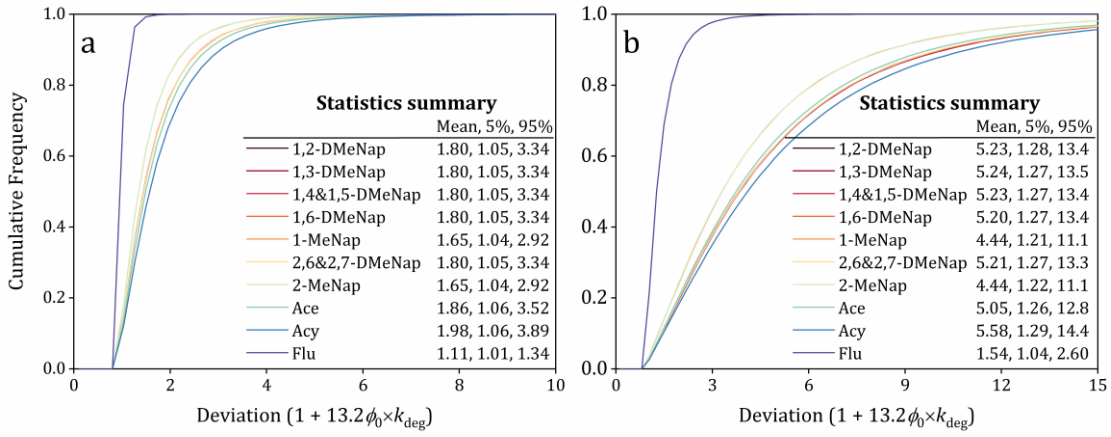

Fig. 4. The impact of the gaseous degradation on K_P' deviation from the equilibrium state estimated based on the Monte Carlo Analysis at −50℃ (a) and 50℃ (b). (Note: The following variables with their distribution patterns and confidence factors (CF) were considered: ϕ_0: uniform distribution, 0 to 1; k_{deg}, lognormal distribution; CF = 3 (Wania and Dugani, 2003).)

4. Implications

According to previous studies, adsorption of gaseous SVOCs onto filters during sampling (Hart and Pankow, 1994) and enhanced adsorption of gaseous SVOCs onto various phases (e.g., soot phase) (Dachs and Eisenreich, 2000) both can influence the equilibrium state of G–P partitioning. Additionally, the present study revealed that the gaseous degradation also caused the deviation of K_P' from the equilibrium state. Therefore, in the present study, the deviation of K_P' from the equilibrium state caused

by these factors were estimated and compared in order to deeply understand the influence of gaseous degradation. As mentioned in above section, the mean deviation resulting from gaseous degradation was estimated (K_P': 1.10 to 5.58 times increased). The deviation caused by the influence of the soot phase within the particles was estimated by averaging the difference between the predictions of the H-B model (Harner and Bidleman, 1998) and the D-E model (Dachs and Eisenreich, 2000) for LMW SVOCs with the range of log K_{OA} from 5 to 9. The increasing times of K_P' caused by the influence of the soot phase within the particles was in the range of 2.68 to 7.70 times. A previous study pointed out that the effect of the adsorption of gaseous SVOCs onto filters could increase K_P' about 1.2 to 1.6 times (Hart and Pankow, 1994). Therefore, it can be found that, the deviation of K_P' from the equilibrium state caused by the gaseous degradation was comparable with that caused by the adsorption of the soot phase, which were both higher than that caused by the adsorption of gaseous SVOCs onto filters. Therefore, it can be concluded that the influence of gaseous degradation should also be considered for the G–P partitioning models of SVOCs, especially for the LMW SVOCs.

5. Limitation

In this study, the gaseous degradation was speculated as the reason for the difference of K_P' for Me-Naps between the daytime and nighttime, which might result in the deviation of K_P' from equilibrium state for LMW SVOCs. In addition, the new steady state G-P partitioning model was used, which demonstrated that the gaseous degradation could deviate the K_P' from equilibrium state. However, there were some limitations in this study. Firstly, the different breakthrough values might occur between the daytime and nighttime, considering their different temperature. The influence of the breakthrough on K_P' was calculated, that could result in 1.20 to 1.27 times higher for K_P' in the daytime than in the nighttime, if the breakthrough (17% to 21%) only occurred

in the daytime, not in the nighttime. However, the increasing of K_P' caused by the breakthrough cannot fully explain the observed diurnal variation with K_P' between daytime and nighttime in this study (2.95 to 4.65 times). Secondly, the present study only considered the gaseous degradation related to the reaction with hydroxyl radicals. However, the gaseous degradation routes, like the other atmospheric oxidation pathways and photodegradation were not included, which may lead to an underestimation of the impact of the total gaseous degradation. Thirdly, the previous studies have demonstrated that PAHs can be entrapped within highly viscous, partially forming secondary organic aerosol particles during particle formation (Zelenyuk et al., 2012; Shrivastava et al., 2017), which could cause the non-exchangeable SVOCs within particles. However, the presence and influence of the non-exchangeable SVOCs within particles on the G–P partitioning behavior were not considered in this study. Therefore, it is imperative to conduct studies for other influencing factors on the G–P partitioning behavior of SVOCs in future, such as the total gaseous degradation, the non-exchangeable SVOCs within particles, and the advection of air masses, among others.

Acknowledgments

This study was supported by the National Natural Science Foundation of China (Nos. 42077341 and 42377377). This study was partially supported by the High-Level Talent Funding Project of Hebei Province, China (B2023003020).

Author contributions

Fu-Jie Zhu: Conceptualization, Methodology, Investigation, Writing – original draft. Zi-Feng Zhang: Writing – review & editing. Li- Yan Liu: Writing – review & editing. Pu-Fei Yang: Writing – review & editing. Peng-Tuan Hu: Writing – review & editing.

Geng-Bo Ren: Writing – review & editing. Meng Qin: Writing – review & editing. Wan-Li Ma: Conceptualization, Methodology, Writing – review & editing.

Appendix A. Supplementary data

Supplementary data for this article can be found at

References

Baskaran, S., Lei, Y. D., and Wania, F.: Reliable prediction of the octanol-air partition ratio, Environmental Toxicology and Chemistry, https://doi.org/10.1002/etc.5201, 2021.

Cao, R., Zhang, H., Geng, N., Fu, Q., Teng, M., Zou, L., Gao, Y., and Chen, J.: Diurnal variations of atmospheric polycyclic aromatic hydrocarbons (pahs) during three sequent winter haze episodes in beijing, china, Science of the Total Environment, 625, 1486-1493, https://doi.org/10.1016/j.scitotenv.2017.12.335, 2018.

Dachs, J. and Eisenreich, S. J.: Adsorption onto aerosol soot carbon dominates gas-particle partitioning of polycyclic aromatic hydrocarbons, Environmental Science & Technology, 34, 3690-3697, https://doi.org/10.1021/es991201, 2000.

Harner, T. and Bidleman, T. F.: Octanol-air partition coefficient for describing particle/gas partitioning of aromatic compounds in urban air, Environmental Science & Technology, 32, 1494-1502, https://doi.org/10.1021/es970890r, 1998.

Hart, K. M. and Pankow, J. F.: High-volume air sampler for particle and gas sampling .2. Use of backup filters to correct for the adsorption of gas-phase polycyclic aromatic-hydrocarbons to the front filter, Environmental Science & Technology, 28, 655-661, https://doi.org/10.1021/es00053a019, 1994.

Hart, K. M., Isabelle, L. M., and Pankow, J. F.: High-volume air sampler for particle and gas sampling. 1. Design and gas sampling performance, Environmental Science & Technology, 26, 1048-1052, https://doi.org/10.1021/es00029a027, 1992.

Hu, P.-T., Ma, W.-L., Zhang, Z.-F., Liu, L.-Y., Song, W.-W., Cao, Z.-G., Macdonald, R. W., Nikolaev, A., Li, L., and Li, Y.-F.: Approach to predicting the size-dependent inhalation intake of particulate novel brominated flame retardants, Environmental Science & Technology, 55, 15236-15245, https://doi.org/10.1021/acs.est.1c03749, 2021.

Hu, P.-T., Su, P.-H., Ma, W.-L., Zhang, Z.-F., Liu, L.-Y., Song, W.-W., Qiao, L.-N., Tian, C.-G., Macdonald, R. W., Nikolaev, A., Cao, Z.-G., and Li, Y.-F.: New equation to predict size-resolved gas-particle partitioning quotients for polybrominated diphenyl ethers, Journal of Hazardous Materials, 400, 123245, https://doi.org/10.1016/j.jhazmat.2020.123245, 2020.

Li, Y., Ma, W., and Yang, M.: Prediction of gas/particle partitioning of polybrominated diphenyl ethers (pbdes) in global air: A theoretical study, Atmospheric Chemistry and Physics, 15, 1669-1681, https://doi.org/10.5194/acp-15-1669-2015, 2015.

Li, Y., Qiao, L., Ren, N., Sverko, E., Mackay, D., and Macdonald, R. W.: Decabrominated diphenyl ethers (bde-209) in chinese and global air: Levels, gas/particle partitioning, and long-range transport: Is long-range transport of bde-209 really governed by the movement of particles?, Environmental Science & Technology, 51, 1035-1042, https://doi.org/10.1021/acs.est.6b05395, 2017.

Li, Y.-F., Qiao, L.-N., Ren, N.-Q., Macdonald, R. W., and Kannan, K.: Gas/particle partitioning of semi-volatile organic compounds in the atmosphere: Transition from unsteady to steady state, Science of The Total Environment, 710, 136394, https://doi.org/10.1016/j.scitotenv.2019.136394, 2020.

Li, Y. F. and Jia, H. L.: Prediction of gas/particle partition quotients of polybrominated diphenyl ethers (pbdes) in north temperate zone air: An empirical approach, Ecotoxicology & Environmental Safety, 108, 65-71, https://doi.org/10.1016/j.ecoenv.2014.05.028, 2014.

Ma, W., Zhu, F., Hu, P., Qiao, L., and Li, Y.: Gas/particle partitioning of pahs based on equilibrium-state model and steady-state model, Science of The Total Environment, 706, 136029, https://doi.org/10.1016/j.scitotenv.2019.136029, 2020.

Ma, W.-L., Zhu, F.-J., Liu, L.-Y., Jia, H.-L., Yang, M., and Li, Y.-F.: Pahs in chinese atmosphere: Gas/particle partitioning, Science of The Total Environment, 693, 133623, https://doi.org/10.1016/j.scitotenv.2019.133623, 2019.

Mackay, D., Celsie, A. K. D., and Parnis, J. M.: Kinetic delay in partitioning and parallel particle pathways: Underappreciated aspects of environmental transport, Environmental Science & Technology, 53, 234-241, https://doi.org/10.1021/acs.est.8b04514, 2019.

Ohura, T., Horii, Y., Kojima, M., and Kamiya, Y.: Diurnal variability of chlorinated polycyclic aromatic hydrocarbons in urban air, japan, Atmospheric Environment, 81, 84-91, https://doi.org/10.1016/j.atmosenv.2013.08.044, 2013.

Qiao, L., Hu, P., Macdonald, R., Kannan, K., Nikolaev, A., and Li, Y.: Modeling gas/particle partitioning of polybrominated diphenyl ethers (pbdes) in the atmosphere: A review, Science of The Total Environment, 729, 138962, https://doi.org/10.1016/j.scitotenv.2020.138962, 2020.

Reisen, F. and Arey, J.: Atmospheric reactions influence seasonal pah and nitro-pah concentrations in the los angeles basin, Environmental Science & Technology, 39, 64-73, https://doi.org/10.1021/es035454l, 2005.

Sadiki, M. and Poissant, L.: Atmospheric concentrations and gas-particle partitions of pesticides: Comparisons between measured and gas-particle partitioning models from source and receptor sites, Atmospheric Environment, 42, 8288-8299, https://doi.org/10.1016/j.atmosenv.2008.07.041, 2008.

Shahpoury, P., Lammel, G., Albinet, A., Sofuoglu, A., Dumanoglu, Y., Sofuoglu, S. C., Wagner, Z., and Zdimal, V.: Evaluation of a conceptual model for gas-particle partitioning of polycyclic aromatic hydrocarbons using polyparameter linear free energy relationships, Environmental Science & Technology, 50, 12312-12319, https://doi.org/10.1021/acs.est.6b02158, 2016.

Shrivastava, M., Lou, S., Zelenyuk, A., Easter, R. C., Corley, R. A., Thrall, B. D., Rasch, P. J., Fast, J. D., Simonich, S. L. M., Shen, H. Z., and Tao, S.: Global long-range transport and lung cancer risk from polycyclic aromatic hydrocarbons shielded by coatings of organic aerosol, Proceedings of the National Academy of Sciences of the United States of America, 114, 1246-1251, https://doi.org/10.1073/pnas.1618475114, 2017.

Ulrich, N., Endo, S., Brown, T. N., Watanabe, N., Bronner, G., Abraham, M. H., and Goss, K.-U.: Ufz-lser database v 3.2.1 [internet], leipzig, germany, helmholtz centre for environmental research-ufz, 2017.

Wang, W., Simonich, S. L. M., Wang, W., Giri, B., Zhao, J., Xue, M., Cao, J., Lu, X., and Tao, S.: Atmospheric polycyclic aromatic hydrocarbon concentrations and gas/particle partitioning at background, rural village and urban sites in the north china plain, Atmospheric Research, 99, 197-206, https://doi.org/10.1016/j.atmosres.2010.10.002, 2011.

Wania, F. and Dugani, C. B.: Assessing the long-range transport potential of polybrominated diphenyl ethers: A comparison of four multimedia models, Environmental Toxicology and Chemistry, 22, 1252-1261, https://doi.org/10.1002/etc.5620220610, 2003.

Wilson, J., Pöschl, U., Shiraiwa, M., and Berkemeier, T.: Non-equilibrium interplay between gas-particle partitioning and multiphase chemical reactions of semi-volatile compounds: Mechanistic insights and practical implications for atmospheric modeling of pahs, Atmospheric Chemistry and Physics, 2020, 1-39, https://doi.org/10.5194/acp-21-6175-2021, 2020.

Zelenyuk, A., Imre, D., Beránek, J., Abramson, E., Wilson, J., and Shrivastava, M.: Synergy between secondary organic aerosols and long-range transport of polycyclic aromatic hydrocarbons, Environmental Science & Technology, 46, 12459-12466, https://doi.org/10.1021/es302743z, 2012.

Zhang, J., Yang, L., Mellouki, A., Chen, J., Chen, X., Gao, Y., Jiang, P., Li, Y., Yu, H., and Wang, W.: Diurnal concentrations, sources, and cancer risk assessments of pm2.5-bound pahs, npahs, and opahs in urban, marine and mountain environments, Chemosphere, 209, 147-155, https://doi.org/10.1016/j.chemosphere.2018.06.054, 2018.

Zhang, X. and McMurry, P. H.: Theoretical analysis of evaporative losses of adsorbed or absorbed species during atmospheric aerosol sampling, Environmental Science & Technology, 25, 456-459, https://doi.org/10.1021/es00015a012, 1991.

Zhu, F., Arina, S., Zhang, Z., Liu, L., Song, W., Cheng, Y., Liu, J., and Ma, W.: Non-equilibrium influence on g/p partitioning of pahs: Evidence from the diurnal and nocturnal variation, Chemosphere, 294, 133722, https://doi.org/10.1016/j.chemosphere.2022.133722, 2022.

Zhu, F.-J., Ma, W.-L., Hu, P.-T., Zhang, Z.-F., and Li, Y.-F.: Temporal trends of atmospheric pahs: Implications for the influence of the clean air action, Journal of Cleaner Production, 296, 126494, https://doi.org/10.1016/j.jclepro.2021.126494, 2021a.

Zhu, F.-J., Ma, W.-L., Zhang, Z.-F., Yang, P.-F., Hu, P.-T., Liu, L.-Y., and Song, W.-W.: Prediction of the gas/particle partitioning quotient of pahs based on ambient temperature, Science of The Total Environment, 811, 151411, https://doi.org/10.1016/j.scitotenv.2021.151411, 2021b.

Zhu, F. J., Hu, P. T., and Ma, W. L.: A new steady-state gas–particle partitioning model of polycyclic aromatic hydrocarbons: Implication for the influence of the particulate proportion in emissions, Atmospheric Chemistry and Physics, 23, 8583-8590, https://doi.org/10.5194/acp-23-8583-2023, 2023.